

Published in final edited form as:

Organometallics. 2012 ; 31(7): 2631–2638. doi:10.1021/om2007453.

Trimethylsilyl-Substituted Hydroxycyclopentadienyl Ruthenium Hydrides as Benchmarks to Probe Ligand and Metal Effects on the Reactivity of Shvo Type Complexes

Charles P. Casey and Hairong Guan

Department of Chemistry, University of Wisconsin-Madison, Madison, Wisconsin 53706

Charles P. Casey: casey@chem.wisc.edu

Abstract

The bis(trimethylsilyl)-substituted hydroxycyclopentadienyl ruthenium hydride [2,5-(SiMe₃)₂-3,4-(CH₂OCH₂)(η⁵-C₄COH)]Ru(CO)₂H (**10**) is an efficient catalyst for hydrogenation of aldehydes and ketones. Because **10** transfers hydrogen rapidly to aldehydes and ketones and because it does not form an inactive bridging hydride during reaction, hydrogenation of aldehydes and ketones can be performed at room temperature under relatively low hydrogen pressure (3 atm); this is a significant improvement compared with previously developed Shvo type catalysts. Kinetic and ²H NMR spectroscopic studies of the stoichiometric reduction of aldehydes and ketones by **10** established a two-step process for the hydrogen transfer: (1) rapid and reversible hydrogen bond formation between OH of **10** and the oxygen of the aldehyde or ketone, (2) followed by slow transfer of both proton and hydride from **10** to the aldehyde or ketone. The stoichiometric and catalytic activities of complex **10** are compared to those of other Shvo type ruthenium hydrides and related iron hydrides.

Metal-ligand bifunctional catalysts¹ for the hydrogenation of polar double bonds provide a “green” alternative to stoichiometric reducing agents such as LiAlH₄ or NaBH₄.² Shvo’s hydroxycyclopentadienyl ruthenium hydride **1** was the first reported metal-ligand bifunctional catalyst;³ it is generated *in situ* by dissociation of the diruthenium bridging hydride **2**, which is itself unreactive towards aldehydes and ketones.⁴ Our group has carried out detailed mechanistic studies of the tolyl analogs of Shvo’s catalytic system. The rates and mechanisms of the steps involved in the catalytic system were separately determined and the kinetics of the overall process was also studied.⁵ A full kinetic model of the hydrogenation based on rate constants for individual steps in the catalysis was developed that simulates the rate of carbonyl compound hydrogenation and of the amounts of ruthenium species **3** and **4** present during hydrogenation (Scheme 1).⁶ Although the reduction of benzaldehyde by ruthenium hydride **3** (the active reducing agent) takes place even at –40 °C in toluene, the partitioning between the inactive diruthenium species **4** and the active monoruthenium hydride **3** dictates the efficiency of the catalytic reaction. At 60 °C, the only observable ruthenium species present during catalytic hydrogenation of aldehydes and ketones was the diruthenium complex **4**. Consequently, the Shvo and related hydrogenation catalysts typically require relatively high temperatures (> 80 °C) in

Correspondence to: Charles P. Casey, casey@chem.wisc.edu.

This article is dedicated to the memory of Gordon Stone, a pioneer in organometallic chemistry.

Supporting Information Available: Preparation of **10-d₂**, **16**, **17**, and **18**; kinetics of reduction of PhCHO by **10**; kinetics of reduction of PhCOMe by ruthenium and iron hydrides; catalytic hydrogenation of carbonyls by **10** and **18**; and X-Ray Crystal Structure of **10**. This material is available free of charge via the Internet at <http://pubs.acs.org>.

combination with high hydrogen pressure (35 atm) to be efficient catalysts for hydrogenation of aldehydes and ketones.

To develop new more active ruthenium catalysts, systems with structures that interfere with the formation of unreactive M–H–M systems but maintain high reactivity of the M–H species are needed. Destabilization of M–H–M formation was achieved by introducing a bulky -NPh group on the Cp ring in place of -OH, but the low NH acidity resulted in slow stoichiometric reduction of carbonyl groups by **5** (Scheme 2).⁷ Protonation of **5** to give **6**, which possesses a much more acidic -NPhH₂⁺ group, gave a very active catalyst, but acid-catalyzed side reactions led to some ether formation.⁷ Complex **7**, in which PPh₃ is substituted for one CO, also prevented formation of unreactive M–H–M complexes.⁸ While **7** is a very selective catalyst for hydrogenation of aldehydes over ketones and a faster catalyst than **4** for aldehyde hydrogenation below 60 °C, it is a slower catalyst at higher temperatures.

Recently, we discovered that the TMS (TMS = trimethylsilyl) substituted hydroxycyclopentadienyl iron hydride **8**, first prepared and fully characterized by Knölker,⁹ is an efficient and chemoselective catalyst for the hydrogenation of ketones (Scheme 3).¹⁰ Kinetics studies have suggested that the hydrogen transfer from hydride **8** to ketones is the turnover-limiting step and the hydrogenation rate is independent on hydrogen pressure. Monitoring the stoichiometric reduction by ¹H NMR and the catalytic hydrogenation by *in situ* IR has shown no evidence of a diiron bridging hydride. Distinctly from all other Shvo type systems mentioned above, this iron hydride catalyzes the hydrogenation of both aldehydes and ketones under mild conditions (25 °C, 3 atm of H₂). Although the reason for no bridging hydride formation is not fully understood, the remarkable reactivity of **8** has prompted us to investigate the chemistry of ruthenium complexes with a similar ligand set.

Here we describe the synthesis of ruthenium hydrides with bis(TMS)-substituted cyclopentadienyl ligands. We have examined their reactivity toward the stoichiometric reduction as well as the catalytic hydrogenation of benzaldehyde and acetophenone. These ruthenium hydrides are far more reactive hydrogenation catalysts than other Shvo type complexes and are similar in reactivity to related iron catalysts.

Results

[2,5-(SiMe₃)₂-3,4-(CH₂OCH₂)(η⁵-C₄COH)]Ru(CO)₂H (**10**)

Reaction of the known ruthenium tricarbonyl⁹ with excess NaOH in THF/H₂O, followed by acidification with H₃PO₄, produced the ruthenium hydride **10** in 73 % yield (Scheme 4). These are the same reaction conditions used by Knölker for the synthesis of iron complex **8**.⁹ The structure of **10** was established spectroscopically and confirmed by X-ray crystallography (Figure 1).

In the X-ray crystal structure of **10**, one of the two CO ligands lies directly below the hydroxyl group on the Cp ring. A similar conformation was observed in the solid-state structure of iron hydride **8**.⁹ In the solid state, each molecule of **10** is linked to two others by hydrogen bonding between the CpOH and the ether oxygen of the fused ring (Figure 2). However, IR and NMR spectroscopy show that **10** exists primarily as a monomer in toluene at 0.01 M. The IR spectrum shows an O—H band at 3591 cm⁻¹, indicative of a non-hydrogen-bonded hydroxyl. The ¹H NMR chemical shift of OH resonance changed from δ 3.56 to δ 3.72¹² upon increasing the concentration of **8** from 0.01 M to 0.10 M; these chemical shifts are consistent with little hydrogen bonding in toluene and with little change in aggregation over this concentration range.

Acidity of the Hydroxyl Proton of **10**

Since the stoichiometric reactivity of CpOH ruthenium hydrides depends strongly on the acidity of the CpOH group, we sought to determine the acidity of the CpOH proton of **10**. The pK_a of **3** (the tolyl analogue of the Shvo hydride) was found to be 17.5 in CH₃CN using Norton's IR method.¹³ The pK_a of PPh₃-substituted hydride **7** was determined to be 20.7.^{8a} The greater acidity of **3** than **7** was correlated with the greater reactivity of **3** in the stoichiometric reduction of aldehydes and ketones.

Norton's IR method was used to determine the pK_a of **10**. When NEt₃ (0.040 M, $pK_a = 18.5$ in CH₃CN) was added to a 0.040 M CH₃CN solution of **10**, IR bands due to **10** at 2014 and 1952 cm⁻¹ decreased in intensity and new bands at 1982 and 1915 cm⁻¹ assigned to NEt₃H⁺{[2,5-(SiMe₃)₂-3,4-(CH₂OCH₂)(η^5 -C₄CO)]Ru(CO)₂H}⁻ (**11**) grew in. The ratio of **11** : **10** was determined to be 1 : 1.8 by comparing the absorbances with independently determined molar absorptivities. The pK_a of **10** was calculated to be 19.0. When 1 equiv of pyridine ($pK_a = 12.4$ in CH₃CN) was added to a CH₃CN solution of **10**, no deprotonation was observed. When 1 equiv of 1,1,3,3-tetramethylguanidine ($pK_a = 23.3$ in CH₃CN) was added to a CH₃CN solution of **10**, complete deprotonation to the guanidinium salt was observed. Ruthenium hydride **10** is 1.5 pK_a units less acidic than hydride **3**, but 1.7 pK_a units more acidic than hydride **7** (Scheme 5).

Stoichiometric Reduction of Benzaldehyde by **10**

The reaction of **10** with excess benzaldehyde in toluene-*d*₈ at -60 °C was monitored by ¹H NMR spectroscopy. Disappearance of the ruthenium hydride resonance of **10** (between $\delta -10.12$ and $\delta -9.65$, *vide infra*) and concurrent appearance of two sets of benzyl alcohol-like resonances were observed. Complete disappearance of **10** was seen within 30 min at -60 °C. Based on the similarity of these two sets of benzyl alcohol-like resonances to those of the iron alcohol complex produced in the reduction of benzaldehyde by iron hydride **8**,¹⁴ they were assigned to two isomeric ruthenium alcohol complexes. The two ruthenium alcohol complexes differ only by hydrogen bonding to the two different oxygens of the Cp ring (Scheme 6). Initially one of the alcohol complexes (presumably **12**) was the dominant species, but slow isomerization led to a 1:1 equilibrium ratio of **12** : **12'**. Above -50 °C, complexes **12** and **12'** decomposed to free benzyl alcohol and some intractable ruthenium species, but no NMR resonances attributable to a diruthenium bridging hydride was observed. The low thermal stability of **12** and **12'** made it impossible to obtain single crystals suitable for X-ray crystallography.

When a solution of **10** in toluene-*d*₈ (0.060 M) was treated with excess benzaldehyde in the presence of PPh₃ at -60 °C, only the alcohol complexes **12** and **12'** were observed; none of the phosphine-trapping product **13** was seen. When the solution was warmed above -50 °C, ruthenium alcohol complexes **12** and **12'** were cleanly converted to a PPh₃-substituted ruthenium complex **13** and the free alcohol (Scheme 7). This establishes that alcohol complexes **12** and **12'** are kinetic products of reduction.

Kinetics of Hydrogen Transfer from **10** to Benzaldehyde

The reaction of **10** (< 0.010 M) with a large excess of PhCHO (> 10 equiv) in toluene-*d*₈ at -60 °C was monitored by ¹H NMR spectroscopy. The peak height of the TMS resonance of **10** relative to that of an internal standard (mesitylene methyl δ 2.15) was followed as a function of time. The disappearance of **10** followed first order kinetics. The observed first order rate constants increased non-linearly as the [PhCHO] increased (Figure 3).

This observation of saturation kinetics supports a mechanism involving rapid pre-equilibrium through hydrogen bonding formation, followed by relatively slow hydrogen

transfer (Scheme 8). It was noted that both the RuH and TMS resonances of **10** shifted relative to solvent residual peak (δ 2.09) during reduction. This is consistent with the presence of a changing ratio of free **10** and **14** (a hydrogen bonded adduct of **10** and PhCHO) during reduction (Scheme 8). The OH resonance of **10/14** was not readily seen in the ^1H NMR spectrum. However, it was possible to observe shifts in the OD resonance in the ^2H NMR spectra of **10-*d*₂/14-*d*₂** during the reaction of **10-*d*₂** with excess PhCHO in toluene. Both the slower reaction of PhCHO with **10-*d*₂** (due to a primary deuterium isotope effect, the reaction was incomplete even after 100 min at -60°C) and the simplified aromatic range in ^2H NMR spectrum provided made these measurements possible. Strong evidence for hydrogen bonding interaction was provided by the shift of the OD resonance from δ 4.7 for pure **10-*d*₂** in toluene to δ 7.8 upon addition of PhCHO.

$$-\frac{d[\text{RuH}]_{\text{total}}}{dt} = k_{\text{obs}}[\text{RuH}]_{\text{total}} = \frac{k_2 K_{\text{eq}}[\text{PhCHO}]}{1 + K_{\text{eq}}[\text{PhCHO}]}[\text{RuH}]_{\text{total}} \quad (1)$$

$$\frac{1}{k_{\text{obs}}} = \frac{1}{k_2} + \frac{1}{k_2 K_{\text{eq}}} \times \frac{1}{[\text{PhCHO}]} \quad (2)$$

The rate law for the mechanism in Scheme 8 is given by eq 1. Manipulation of eq 1 gives eq 2, which predicts a linear relationship between $1/k_{\text{obs}}$ with $1/[\text{PhCHO}]$. Such a relationship was observed (Figure 4). K_{eq} and k_2 were determined to be $9.3 \pm 1.1 \text{ M}^{-1}$ and $3.0 \pm 0.1 \times 10^{-3} \text{ s}^{-1}$ from the slope and intercept of Figure 4.

The kinetics of the reaction of **10** ($< 0.010 \text{ M}$) with a large excess of PhCHO (> 10 equiv) in toluene-*d*₈ was measured over a range of [PhCHO] concentrations between -68 and -54°C to obtain the equilibrium constants K_{eq} and rate constants k_2 as a function of temperature. A van't Hoff plot gave $\Delta H^\circ = -8.5 \pm 1.7 \text{ kcal mol}^{-1}$ and $\Delta S^\circ = -35.9 \pm 8.2 \text{ eu}$ for the hydrogen bonding formation; and an Eyring plot gave $\Delta H^\ddagger = 13.3 \pm 1.3 \text{ kcal mol}^{-1}$ and $\Delta S^\ddagger = -6.7 \pm 6.2 \text{ eu}$ for the hydrogen transfer step. The large negative entropy ΔS° is consistent with the hydrogen-bonding formation that brings **10** and PhCHO together prior to hydrogen transfer.

Stoichiometric Reduction of Acetophenone by **10**

Reduction of acetophenone by **10** was much slower than reduction of benzaldehyde and took place at 5°C with or without a trapping agent to give free 1-phenylethanol. In the presence of PPh_3 , complex **13** was the only observed ruthenium product; in the absence of any external ligand, a complicated mixture of ruthenium species was obtained. In both cases, no bridging hydride was detected.

Kinetics of Hydrogen Transfer from **10** to Acetophenone

Similar to benzaldehyde reduction, the rate of hydrogen transfer from **10** to acetophenone in the presence of PPh_3 exhibited a first order in hydride, and kinetic saturation in acetophenone (Figure S6, supporting information). The chemical shift of the ruthenium hydride shifted during the course of reduction, consistent with a changing ratio of free **10** and **15** (a hydrogen bonded adduct of **8** and PhCOMe). The equilibrium constant K_{eq} for

hydrogen bond formation and the rate constant k_2 for hydrogen transfer step were determined to be $5.7 \pm 1.6 \text{ M}^{-1}$ and $3.7 \pm 0.5 \times 10^{-3} \text{ s}^{-1}$ respectively at 5°C .

Using the measured $\Delta H^\circ = -8.5 \pm 1.7 \text{ kcal mol}^{-1}$ and $\Delta S^\circ = -35.9 \pm 8.2 \text{ eu}$ for the hydrogen bond formation between **10** and benzaldehyde, K_{eq} was estimated to be 0.068 at 5°C , which corresponds to only about 1.3% **14** in the presence of 0.2 M PhCHO. This corresponds to an 84 fold smaller K_{eq} for benzaldehyde compared with acetophenone. If this is entirely an enthalpic effect, it is consistent with a $2.4 \text{ kcal mol}^{-1}$ stronger hydrogen bond to the ketone compared with the aldehyde. Ketones ($\text{p}K_{\text{a}}$ of protonated PhCOMe is 5.2) are known to be significantly stronger bases than aldehydes ($\text{p}K_{\text{a}}$ of protonated PhCHO is 6.7).¹⁵

Comparison of Kinetics of Reduction by Iron and Ruthenium Hydrides

The observation of saturation kinetics for the reduction of acetophenone by ruthenium hydride **10** and the evidence for a hydrogen bonded adduct between **10** and acetophenone stands in strong contrast with the reduction of acetophenone by iron hydride **8**, which showed simple first order dependence on both acetophenone and **8**.¹⁰ In addition, no significant chemical shift change was observed for OD resonance in the ^2H NMR spectrum after addition of excess PhCHO or acetophenone to solutions of **8-d₂** in toluene if contrast to the substantial shifts for ruthenium hydride **10-d₂**.

This discrepancy could be due to differences between the metals (Fe or Ru) or differences between the Cp ligands (with or without ether linkage). To separate these two effects, an iron hydride **16** with the same ligand set as ruthenium hydride **10** was synthesized and the kinetics of hydrogen transfer from **16** to acetophenone were examined (Scheme 9).¹⁶ As with **10**, the reduction of acetophenone by **16** showed a first order dependence on hydride **16**, and saturation dependence on acetophenone (supporting material, Figure S7).

Since the strength of a hydrogen bond correlates with the acidity of the hydrogen donor, we determined the acidity of the OH proton of **16** using the IR method. The $\text{p}K_{\text{a}}$ of iron complex **16** was found to be 19.0, the same as that of analogous ruthenium complex **10**, establishing that the metal had little influence on the acidity. In contrast, replacing the oxygen-containing five-membered ring in iron complex **16** with an all-carbon six-member ring decreased the OH proton acidity; the $\text{p}K_{\text{a}}$ value of OH proton in **8** was found to be 20.6. Apparently the electron withdrawing ether oxygen increases the acidity of the CpOH group of **16** relative to **8**. In accordance with the $\text{p}K_{\text{a}}$ values, the hydride complexes **10** and **16** with the more acidic CpOH protons are prone to form hydrogen-bonded intermediates before transfer of hydrogens. In contrast, the less acidic CpOH proton of **8** does not lead to an observable hydrogen bonded intermediate and proton transfer and hydride transfer take place simultaneously.

Synthesis of the Ruthenium Analog **18** of Iron Complex **8**

The ruthenium analog $[2,5-(\text{SiMe}_3)_2\text{-}3,4\text{-}[(\text{CH}_2)_4](\eta^5\text{-C}_4\text{COH})]\text{Ru}(\text{CO})_2\text{H}$ (**18**) related to iron complex **8** was synthesized for comparison (Scheme 10). For unknown reasons, ruthenium hydride **18** was always contaminated with small amounts ($< 10 \text{ mol } \%$) of a bridging hydride complex. The reaction of **18** with PhCHO in toluene- d_8 at -60°C generated a single alcohol complex **19** (there is only one oxygen available for intramolecular hydrogen bonding, but two oxygens are available in **12** and **12'**).

Ketone and Aldehyde Hydrogenation Catalyzed by Ruthenium Hydrides **10** and **18**

Having established that the stoichiometric reduction of carbonyls by **10** occurred at low temperature and that no inactive bridging hydride was generated during these reactions, we

anticipated that **10** might serve as an aldehyde and ketone hydrogenation catalyst under mild conditions. Indeed, the hydrogenation of acetophenone (0.3 M in toluene) was catalyzed by **10** (2 mol %) at 25 °C under 35 atm of H₂. The exponential disappearance of acetophenone (1690 cm⁻¹) was monitored using a ReactIR apparatus; the only observed ruthenium species was **10** (2020 and 1960 cm⁻¹).¹⁷ The half-life of the hydrogenation was determined to be 1.9 h. A similar hydrogenation was also carried out under much lower hydrogenation pressure (3 atm) using a Fisher-Porter apparatus, and reaction progress was periodically monitored by taking ¹H NMR spectrum of the aliquots withdrawn from the reaction mixture. A half-life of 2.0 h was determined, suggesting that the rate of hydrogenation was independent on H₂ pressure. The hydrogenation product 1-phenylethanol was isolated in 80 % yield after 20 h of hydrogenation (Table 1).

The hydrogenation of benzaldehyde catalyzed by **10** was more rapid. With the same concentration of substrate and catalyst loading under 3 atm of H₂ pressure, the reaction was complete within one hour. The hydrogenation product benzyl alcohol was isolated in 91 % yield.

Although a small amount of bridging hydride was always seen during the synthesis and reactions of hydride **18**, the hydrogenation of carbonyls catalyzed by **18** was reasonably efficient. The catalytic activity of ruthenium complex **18** was comparable to that of iron complex **8**¹⁰ (Table 1).

Discussion

In an effort to develop a more active ruthenium hydrogenation catalyst related to the Shvo system, we synthesized the bis(trimethylsilyl) substituted Cp complex **10** in a successful effort to avoid formation of unreactive bridging hydrides analogous to **2** and **4**. Since we have not seen detectable amounts of bridging hydrides related to either bis(trimethylsilyl)-substituted Cp iron complex **8** or ruthenium complex **10**, we suggest that the sterically large TMS groups prevent formation of bridging hydrides. The reduction of carbonyls catalyzed by **10** is fast at low temperature; under H₂ atmosphere, we suggest that a coordinatively unsaturated species is generated and rapidly trapped by hydrogen to regenerate the hydride catalyst (Scheme 11). With sufficient H₂ present, the hydrogenation is independent on the H₂ pressure and the turnover-limiting step is the hydrogen transfer step.

Experimental Evidence for a Hydrogen Bonded Intermediate Prior to Hydride Transfer from **10**

The stoichiometric reduction of PhCHO by **10** displayed saturation kinetics that provided the first direct evidence for the hydrogen bonded adduct **14** prior to hydride transfer. Substantial shifts of NMR resonances of **10** upon addition of PhCHO also supported the formation of the hydrogen-bonded complex **14**. The K_{eq} values determined from the saturation kinetics analysis indicate that at -60 °C about 60% of the ruthenium species present at 0.2 M PhCHO is the hydrogen bonded adduct **14**. This is the first system in which a hydrogen-bonded CpOH--O=CHR interaction has been directly seen. Why wasn't it seen before for other Ru and Fe complexes? We suggest that this is related to the higher acidity of the CpOH group of **10** compared with iron complex **8** and other Ru complexes such as **7**. The greater acidity of **10** results in a stronger hydrogen bond to the carbonyl group. The greater acidity also increases the reactivity of **10**; the faster rate of reaction of **10** allows kinetic measurements at lower temperatures where the hydrogen-bonded adduct **14** is more thermodynamically stable (the large negative $\Delta S^\circ = -36$ eu diminishes K_{eq} as the temperature is increased).

Overall, a wide range of subtle differences in kinetic behavior has been seen for the transfer of hydride and proton from species related to the Shvo catalyst. In the case of **10**, there is rapid and reversible formation of substantial amounts of hydrogen-bonded intermediate **14** prior to hydride and proton transfer. In the case of **2**, computations suggest the reversible formation of substantial amounts of hydrogen-bonded intermediate, but not enough of it is formed to obtain direct experimental evidence for its presence.¹⁸ In the case of reduction of *p*-MeO-C₆H₄CMe=N-Ph by **1**, the absence of a $k_{\text{OH}}/k_{\text{OD}}$ isotope effect was interpreted as resulting from proton transfer to nitrogen occurring prior to rate limiting hydride transfer.¹⁹ In the case of reduction of TolCH=N-CHMe₂ by **3**, both substrate isomerization and inverse isotope effects provided information that both proton and hydride transfer were rapid and reversible and amine coordination to Ru was rate limiting.²⁰

Comparison of Stoichiometric Reduction Rates of **10** and other Hydrides

The rate constants and activation parameters determined previously^{5,6,10} allow comparison of the reactivity of hydride **10** and related hydrides. For benzaldehyde at -60 °C, hydride **10** is about 20–40 times more reactive than the tolyl analog of Shvo's hydride **3** and is significantly more reactive than PPh₃-substituted hydride **7** (Scheme 12). Interestingly, for acetophenone reduction at 5 °C, hydride **10** is 4–8 times less reactive than **3**; however, it is comparable to **8** and slightly more reactive than the iron analog **16** (Scheme 13). There is almost no reaction between **7** and acetophenone at 5 °C. The close similarity of the rates for analogous Fe and Ru complexes **8** and **10** is very significant. It suggests that the more economical iron catalysts are attractive alternatives to ruthenium catalysts.

Comparison of Catalytic Reactivity of **10** and Other Hydrides

The activity of catalysts related to the Shvo system depend not only on their stoichiometric reduction rates, but also on whether the dominant species is an active monoruthenium hydride or an unreactive bridging hydride. For example, PPh₃-substituted hydride **7** catalyzes the hydrogenation of PhCHO at room temperature under 2.5 atm of H₂ pressure, while hydride **3** is completely unreactive under similar conditions. While **3** is a faster stoichiometric hydrogen donor than **7**, it is a slow catalyst because it is rapidly converted to the inactive diruthenium hydride **4**. The ruthenium hydrides **10** and **18** reported here are highly active catalysts both because of rapid stoichiometric rates and because they are present as active monoruthenium species. The hydrogenation of PhCHO catalyzed by **10** or **18** is complete within 1 h at 25 °C under 3 atm of H₂ pressure as opposed to 20 h for **7** (Scheme 14). More remarkably, the hydrogenation of acetophenone catalyzed by **10** or **18** takes place at room temperature and low H₂ pressure (3 atm); previously developed Shvo type ruthenium catalysts are ineffective under these mild conditions.

Experimental Section

General Procedures

All air-sensitive compounds were prepared and handled under a nitrogen atmosphere using standard Schlenk and inert-atmosphere glove box techniques. Toluene was deoxygenated and dried in a solvent purification system by passing through an activated alumina column and an oxygen-scavenging column under nitrogen.²¹ Toluene-*d*₈ and C₆D₆ were distilled from Na and benzophenone under a nitrogen atmosphere. CH₃CN and Et₃N were dried over CaH₂ and distilled under a nitrogen atmosphere. Methanol, glyme, and benzene were degassed by bubbling N₂ through the solvents for 15 min before use. {2,5-(SiMe₃)₂-3,4-[(CH₂)₄](η⁵-C₄COH)}Fe(CO)₂H (**8**),⁹ [2,5-(SiMe₃)₂-3,4-(CH₂OCH₂)(η⁴-C₄CO)]Ru(CO)₃ (**9**),¹¹ 2,5-(SiMe₃)₂-3,4-[(CH₂)₄](C₄CO),²² Me₃SiC≡C(CH₂)₄C≡CSiMe₃,²³ and [2,5-(SiMe₃)₂-3,4-(CH₂OCH₂)(η⁴-C₄CO)]Fe(CO)₃²⁴ were prepared as described in the literature.

[2,5-(SiMe₃)₂-3,4-(CH₂OCH₂)(η⁵-C₄COH)]Ru(CO)₂H (**10**)

Under a nitrogen atmosphere, a degassed solution of NaOH (0.80 g, 20 mmol) in 25 mL of H₂O was added to a solution of **9** (1.13 g, 2.5 mmol) in 50 mL THF. The resulting biphasic mixture was vigorously stirred at room temperature for 2.5 h before 85 wt. % of H₃PO₄ in H₂O (about 0.8 mL) was added to neutralize the reaction mixture. The organic layer was transferred via cannula into a Schlenk flask under nitrogen and the aqueous layer was extracted with Et₂O several times. The combined organic layers were concentrated under vacuum, dissolved in degassed benzene, dried over Na₂SO₄, and filtered into another Schlenk flask. The resulting solution was pumped to dryness to afford **10** as a yellow powder (0.78 g, 73% yield). X-ray quality crystals of **10** were grown via slow diffusion of hexanes into a saturated solution of **10** in CH₂Cl₂ at -30 °C. ¹H NMR (toluene-*d*₈, 300 MHz) δ -10.12 (s, RuH, 1H), 0.17 (s, Si(CH₃)₃, 18H), 3.58 (br s, OH, 1H), 4.28–4.58 (m, CH₂, 4H). ¹³C{¹H} NMR (toluene-*d*₈, 126 MHz) δ 0.35 (Si(CH₃)₃), 68.31 (CH₂), 70.99, 111.07, 151.31 (COH), 201.43 (Ru(CO)₂). IR (toluene, cm⁻¹) 2018, 1959. HRMS (ESI) calcd (found) for [C₁₅H₂₄O₄Si₂Ru+Na]⁺ 449.0154 (449.0174).

pK_a Determination of CpOH Proton of **10**

Triethylamine (2.8 μL, 20 μmol) was mixed with a solution of **10** (8.5 mg, 20 μmol) in CH₃CN (500 μL). An aliquot of the solution was syringed into a 0.1 mm CaF₂ IR cell. Two resonances at 2014 and 1952 cm⁻¹ were assigned to **10** and two at 1982 and 1915 cm⁻¹ were assigned to NET₃H⁺[2,5-(SiMe₃)₂-3,4-(CH₂OCH₂)(η⁵-C₄CO)]Ru(CO)₂H⁻ (**11**). The absolute concentrations of the two species were determined by obtaining the molar absorptivities of **10** and **11**. For **10**: 2014 (1640 M⁻¹ cm⁻¹) and 1952 cm⁻¹ (1800 M⁻¹ cm⁻¹). For **11**: 1982 (1480 M⁻¹ cm⁻¹) and 1915 cm⁻¹ (1670 M⁻¹ cm⁻¹).²⁵ From the molar absorptivities, the ratio of **10** : **11** was determined to be 1.8 : 1. By using the known pK_a of NET₃ (pK_a = 18.5) and the observed equilibrium constant (K_{eq} = 0.30), a pK_a of 19.0 was determined for the CpOH proton of **10**.

Stoichiometric Reduction of Benzaldehyde by **10**

A Teflon capped NMR tube containing a solution of **10** (12.6 mg, 30 μmol) in toluene-*d*₈ (400 μL) was chilled in a dry ice/acetone bath, and a solution of PhCHO (3.6 μL, 36 μmol) in toluene-*d*₈ (100 μL) was added *via* a gas tight syringe through the Teflon cap. The two solutions were carefully mixed while cold, and the NMR tube was immediately placed into an NMR probe at -60 °C (calibrated). The progress of reduction was monitored by ¹H NMR spectroscopy. After 30 min, almost all **10** had disappeared and two sets of peaks corresponding to ruthenium alcohol complexes **12** and **12'** grew in. The major complex slowly isomerized to the minor complex, and finally reached an equilibrium ratio of 1 : 1. Major alcohol complex **12**: ¹H NMR (toluene-*d*₈, 360 MHz) δ 0.33 (s, Si(CH₃)₃, 18H), 3.82 and 4.14 (AB, J_{AB} = 10.8 Hz, CH₂, 4H), 4.03 (s, PhCH₂OH, 2H), 6.67–7.43 (m, Ar, 5H), and OH resonance was not located. Minor alcohol complex **12'**: ¹H NMR (toluene-*d*₈, 360 MHz) δ 0.25 (s, Si(CH₃)₃, 18H), 3.97 and 4.37 (AB, J_{AB} = 10.8 Hz, CH₂, 4H), 4.41 (s, PhCH₂OH, 2H), 6.67–7.43 (m, Ar, 5H), and OH resonance was not located.

NMR Measurements of Rate Constants for the Reduction of Benzaldehyde by **10**

Under a nitrogen atmosphere a solution of PhCHO (1.0 M) in toluene-*d*₈ was mixed with a solution of **10** and mesitylene (internal standard) in a resealable NMR tube at -78 °C. The first ¹H NMR spectrum was recorded within 5 min of mixing, and the reaction was monitored for three to five half-lives. Zero filling was used to ensure adequate digital resolution. The height of the Si(CH₃)₃ resonance of **10** (which steadily shifted from δ 0.34 to δ 0.38) was compared to that of mesitylene (δ 2.15). The NMR probe temperature was

calibrated using a 100 % methanol standard.²⁶ The results are summarized in Tables S1–S5 and S1–S5 in the supporting information.

Supplementary Material

Refer to Web version on PubMed Central for supplementary material.

Acknowledgments

Financial support from the Department of Energy, Office of Basic Energy Sciences is gratefully acknowledged. Grants from NSF (CHE-9208463 and CHE-9709065) and NIH (1 S10 RR0 8389-01) for the purchase of NMR spectrometers are acknowledged. We thank Dr. Ilia Guzei for assistance with X-ray crystallography and Dr. Charles Fry for assistance with NMR spectroscopy.

References

1. Noyori introduced this nomenclature for catalysts that transfer a hydride from a metal center and a proton from a ligand. Yamakawa M, Ito H, Noyori R. *J. Am. Chem. Soc.* 2000; 122:1466.
2. Fehring V, Selke R. *Angew. Chem. Int. Ed.* 1998; 37:1827.
3. (a) Shvo Y, Czarkie D, Rahamim Y, Chodosh DF. *J. Am. Chem. Soc.* 1986; 108:7400.(b) Menashe N, Shvo Y. *Organometallics.* 1991; 10:3885.(c) Menashe N, Salant E, Shvo Y. *J. Organomet. Chem.* 1996; 514:97.
4. For recent reviews of Shvo's Catalyst: Warner MC, Casey CP, Bäckvall J-E. *Top. Organomet. Chem.* 2011; 37:85. Conley BL, Pennington-Boggio MK, Boz E, Williams TJ. *Chem. Rev.* 2010; 110:2294. [PubMed: 20095576]
5. (a) Casey CP, Singer SW, Powell DR, Hayashi RK, Kavana M. *J. Am. Chem. Soc.* 2001; 123:1090. [PubMed: 11456662] (b) Casey CP, Johnson JB, Singer SW, Cui Q. *J. Am. Chem. Soc.* 2005; 127:3100. [PubMed: 15740149] (c) Casey CP, Johnson JB. *Can. J. Chem.* 2005; 83:1339.
6. Casey CP, Beetner SE, Johnson JB. *J. Am. Chem. Soc.* 2008; 130:2285. [PubMed: 18215043]
7. Casey CP, Vos TE, Singer SW, Guzei IA. *Organometallics.* 2002; 21:5038.
8. (a) Casey CP, Strotman NA, Beetner SE, Johnson JB, Priebe DC, Vos TE, Khodavandi B, Guzei IA. *Organometallics.* 2006; 25:1230.(b) Casey CP, Strotman NA, Beetner SE, Johnson JB, Priebe DC, Guzei IA. *Organometallics.* 2006; 25:1236.
9. Knölker HJ, Baum E, Goesmann H, Klauss R. *Angew. Chem. Int. Ed.* 1999; 38:2064.
10. Casey CP, Guan H. *J. Am. Chem. Soc.* 2007; 129:5816. [PubMed: 17439131]
11. Yamamoto Y, Miyabe Y, Itoh K. *Eur. J. Inorg. Chem.* 2004:3651.
12. This chemical shift change amounts to 48 Hz using a 300 MHz NMR spectrometer.
13. (a) Jordan RF, Norton JR. *J. Am. Chem. Soc.* 1982; 104:1255.(b) Moore EJ, Sullivan JM, Norton JR. *J. Am. Chem. Soc.* 1986; 108:2257. [PubMed: 22175569]
14. Casey CP, Guan H. *J. Am. Chem. Soc.* 2009; 131:2499. [PubMed: 19193034]
15. Arnett EM, Quirk RP, Larsen JW. *J. Am. Chem. Soc.* 1970; 92:3977.
16. The reduction of PhCHO by iron hydrides **8** and **16** were fast even at -72 °C. The rates were not measured with accuracy.
17. Based on Figure S4, Keq for acetophenone at 25 °C is expected to be small, and the reduction could be first order dependent on both hydride **10** and the ketone.
18. (a) Casey CP, Bikzhanova GA, Cui Q, Guzei IA. *J. Am. Chem. Soc.* 2005; 127:14062. [PubMed: 16201828] (b) Comas-Vives A, Ujaque G, Lledós A. *Organometallics.* 2007; 26:4135.
19. (a) Samec JSM, Éll AH, Åberg JB, Privalov T, Eriksson L, Bäckvall J-E. *J. Am. Chem. Soc.* 2006; 128:14293. [PubMed: 17076502] (b) Éll AH, Johnson JB, Bäckvall JE. *Chem. Commun.* 2003:1652.
20. Casey CP, Johnson JB. *J. Am. Chem. Soc.* 2005; 127:1883. [PubMed: 15701023]
21. Pangborn AB, Giardello MA, Grubbs RH, Rosen RK, Timmers FJ. *Organometallics.* 1996; 15:1518.

22. Takahashi T, Tsai FY, Li Y, Nakajima K. *Organometallics*. 2001; 20:4122.
23. Bushnell LPM, Evitt ER, Bergman RG. *J. Organomet. Chem.* 1978; 157:445.
24. (a) Knölker HJ, Heber J, Mahler CH. *Synlett*. 1992:1002.(b) Knölker HJ, Heber J. *Synlett*. 1993:924.
25. The molar absorptivities of the 1,1,3,3-tetramethylguanidinium salt (1976 and 1908 cm^{-1}) were used to determine the concentration of **11**.
26. (a) van Geet AL. *Anal. Chem.* 1970; 42:679.(b) Raidford DS, Fisk CL, Becker ED. *Anal. Chem.* 1979; 51:2050.

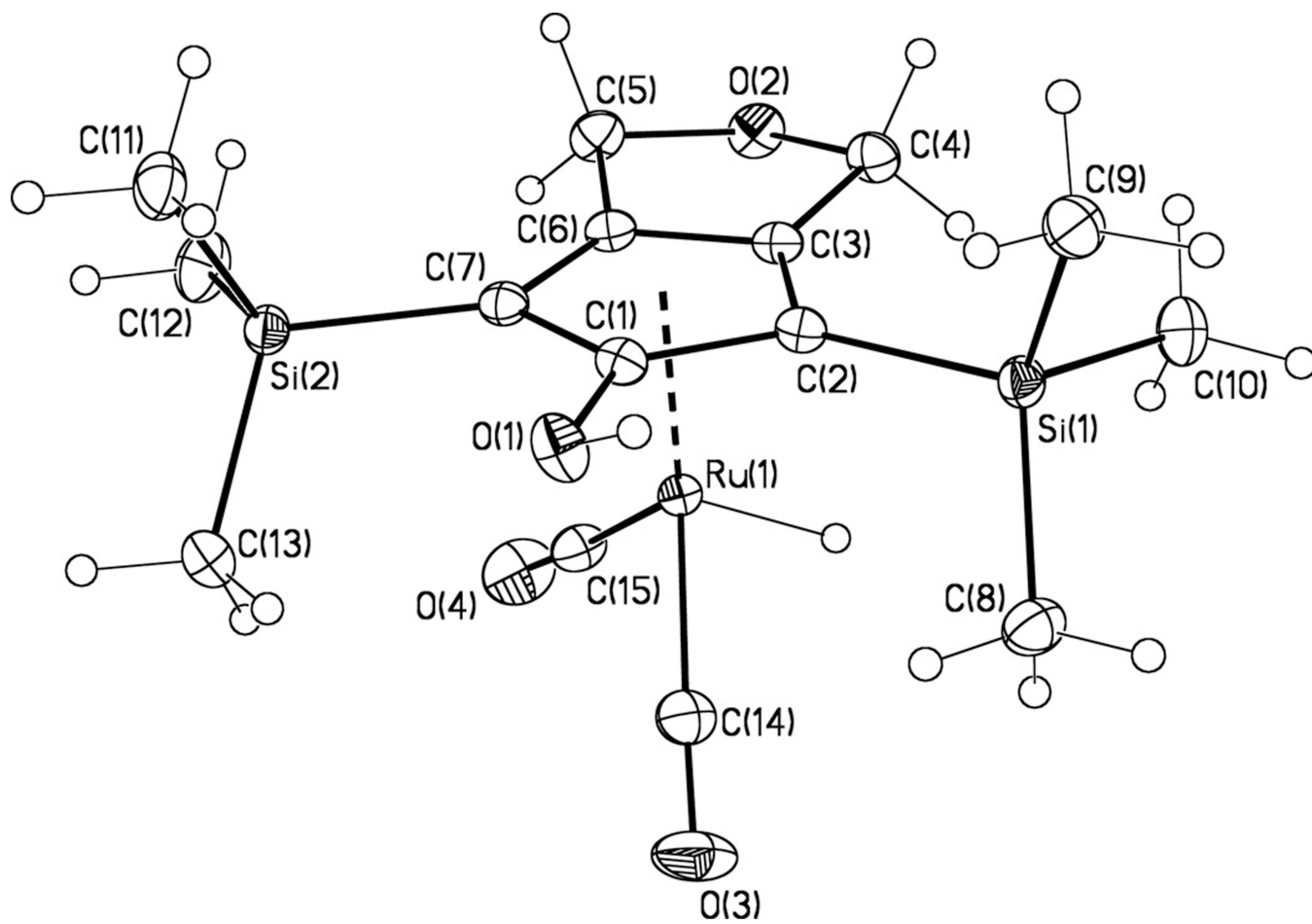


Figure 1.
X-Ray crystal structure of **10** shown with 50% probability ellipsoids.

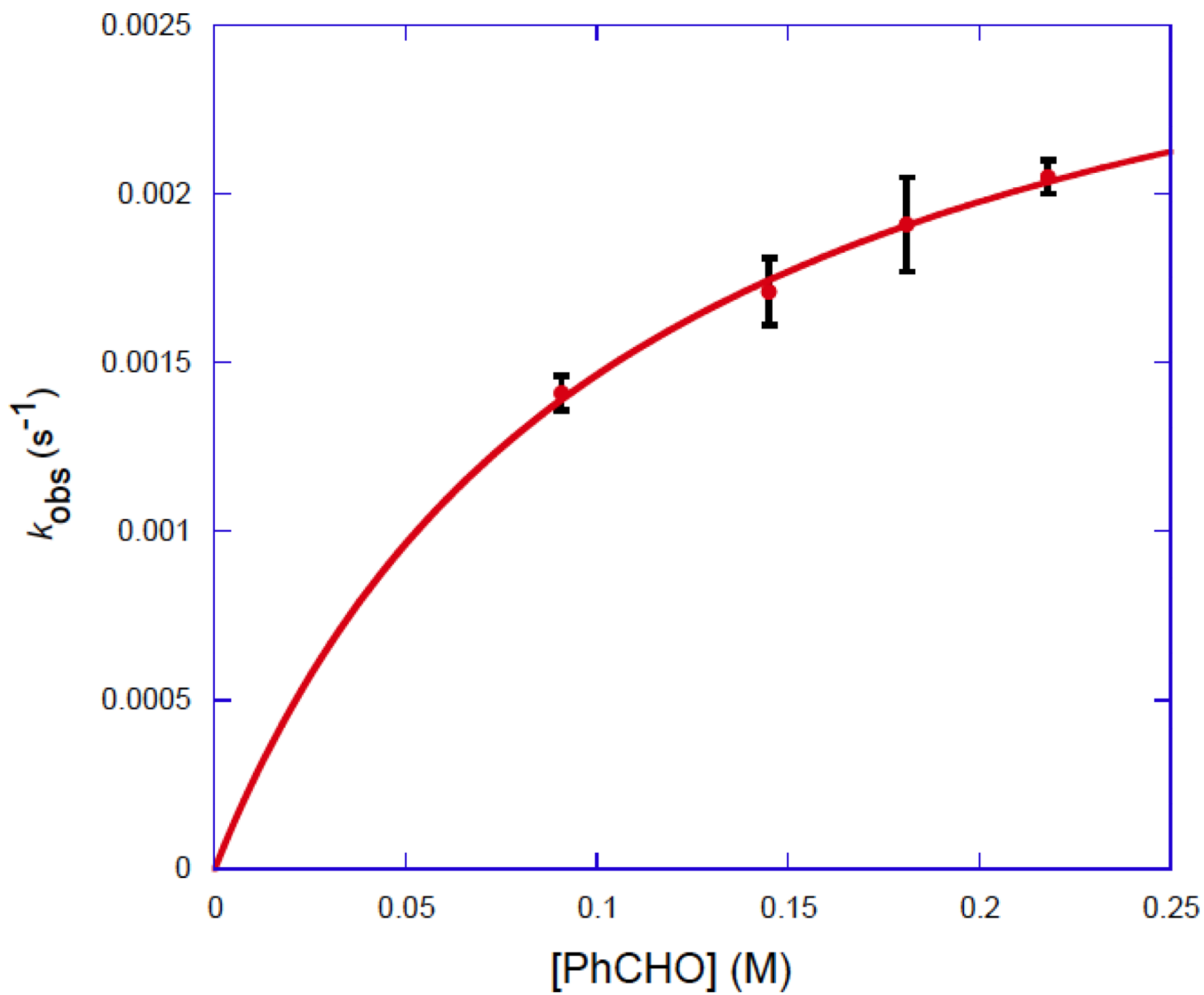


Figure 3. Plot of k_{obs} for reduction of PhCHO by **10** vs. [PhCHO] in toluene- d_8 at -60 °C.

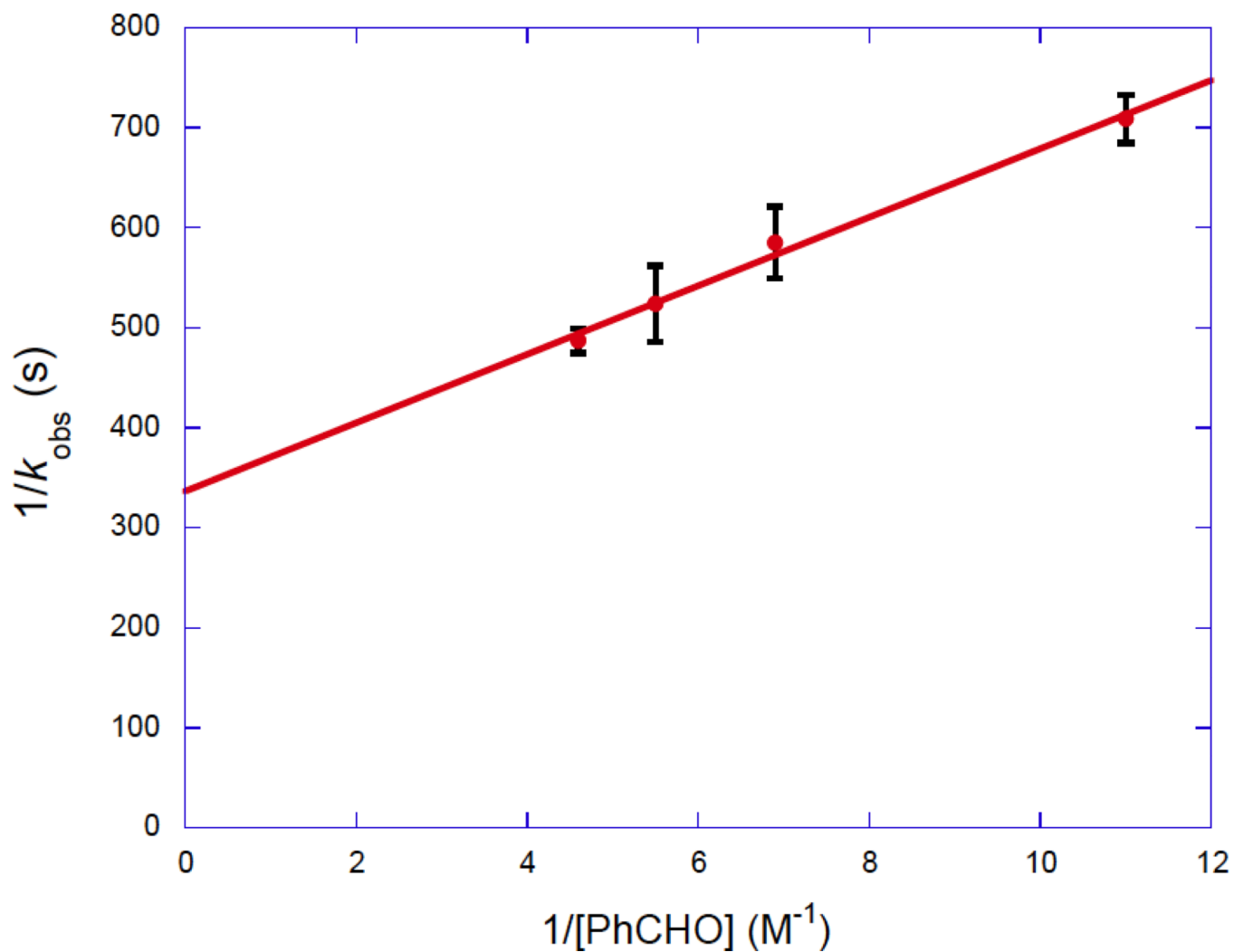
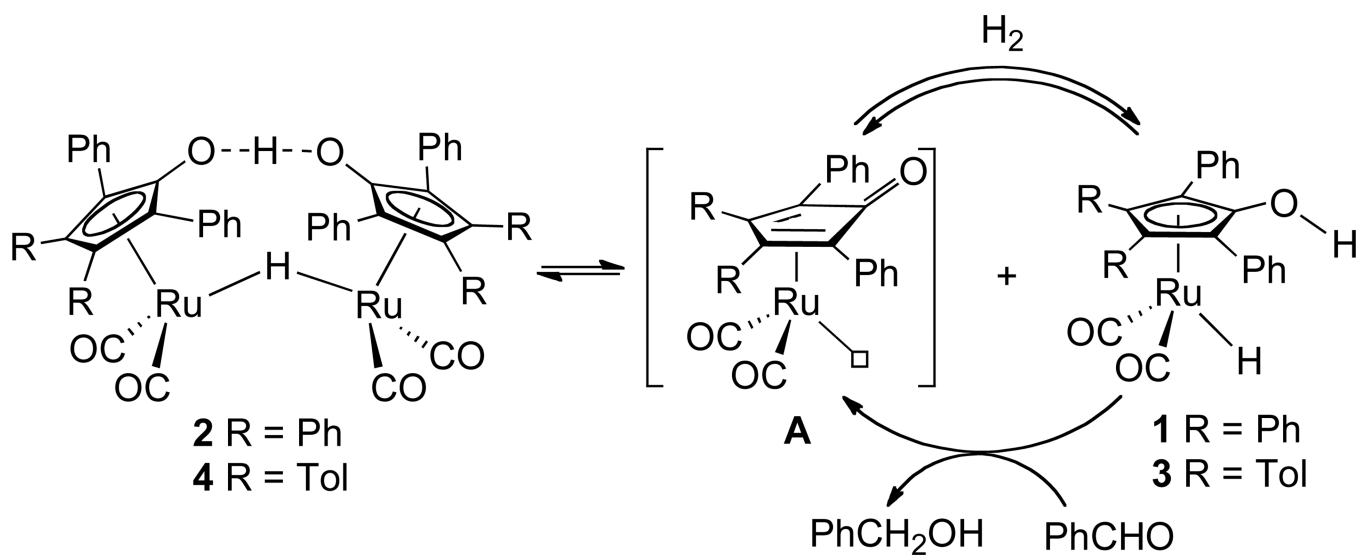
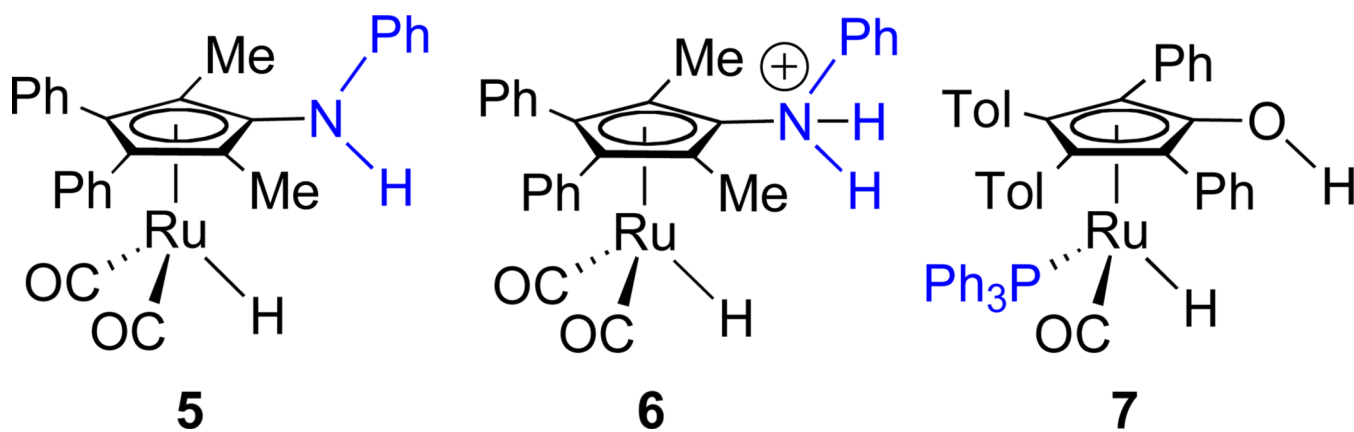


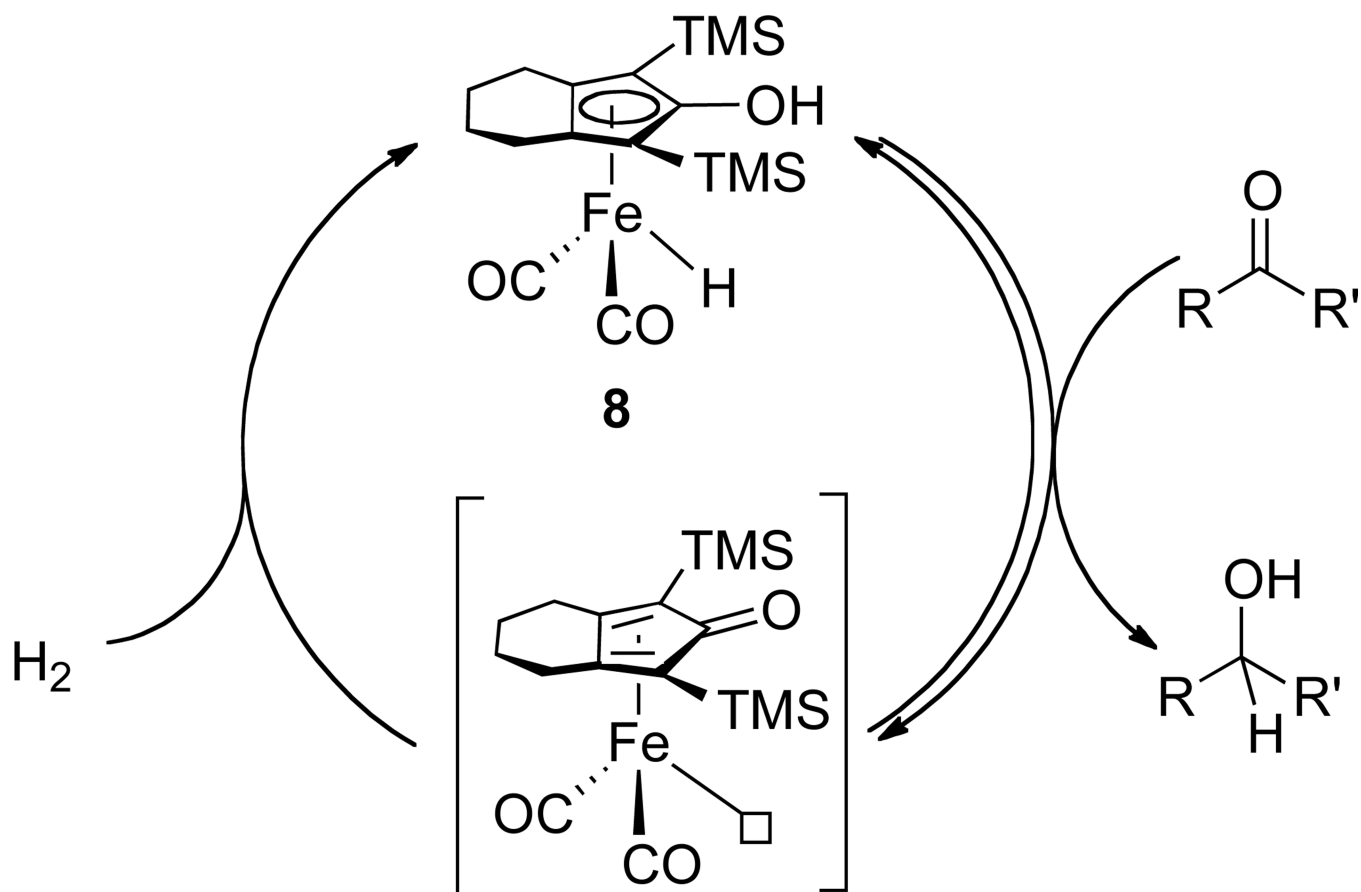
Figure 4. Plot of $1/k_{\text{obs}}$ as a function of $1/[\text{PhCHO}]$ in toluene- d_8 at $-60 \text{ }^\circ\text{C}$.



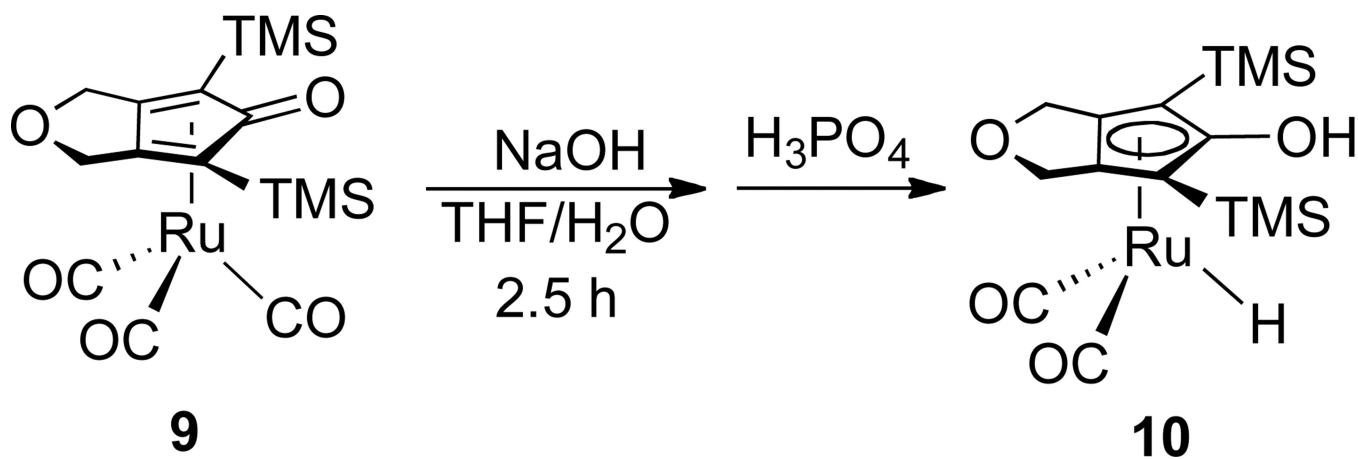
Scheme 1.



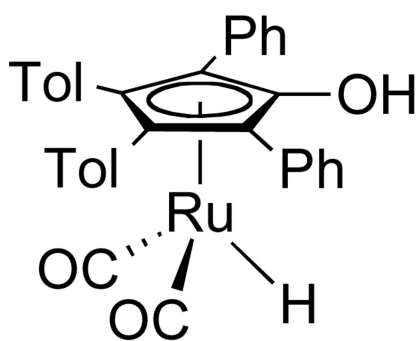
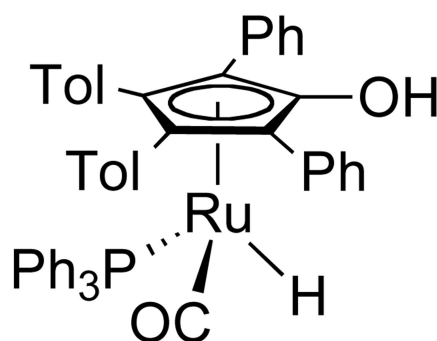
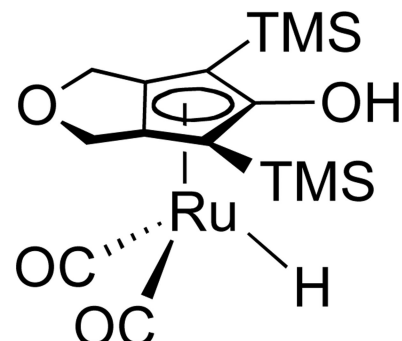
Scheme 2.



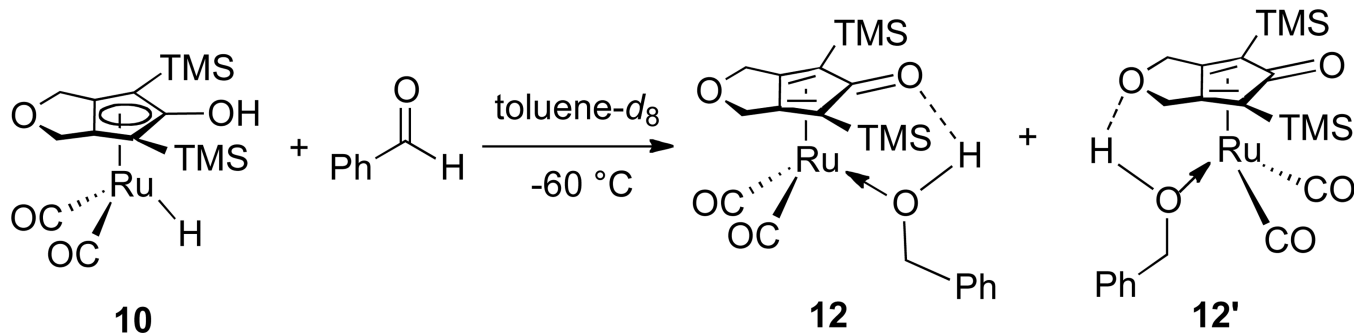
Scheme 3.



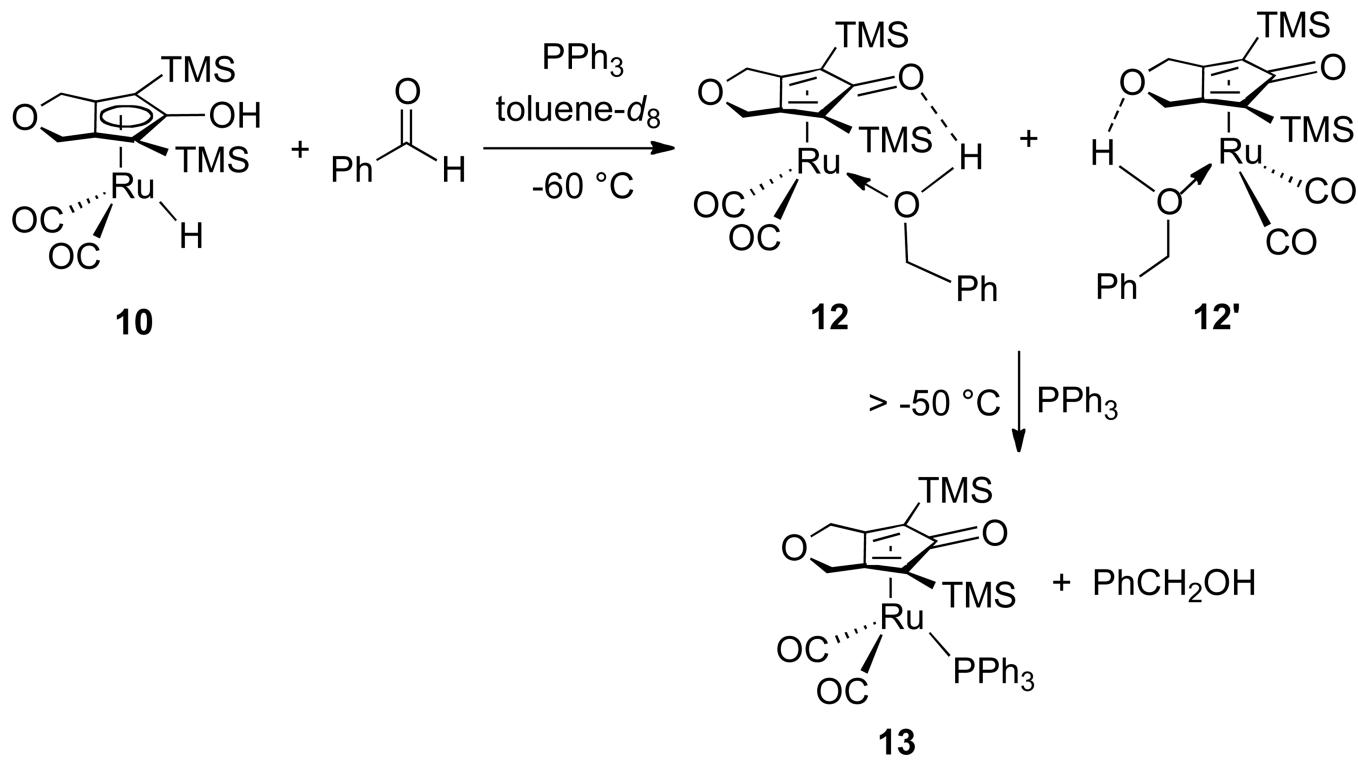
Scheme 4.

**3** pK_a 17.5**7** pK_a 20.7**10** pK_a 19.0

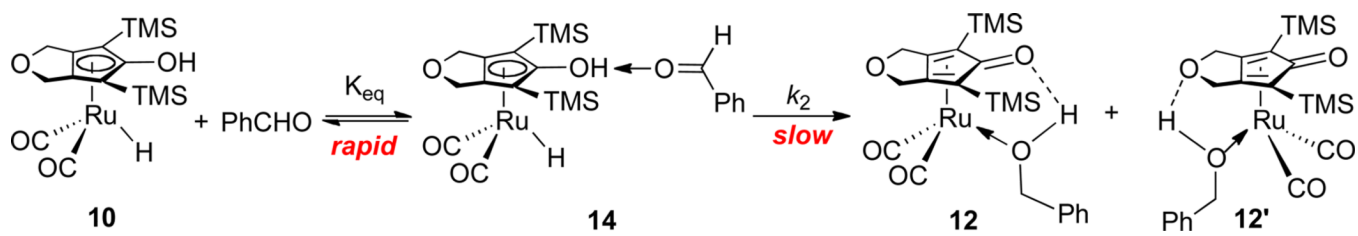
Scheme 5.



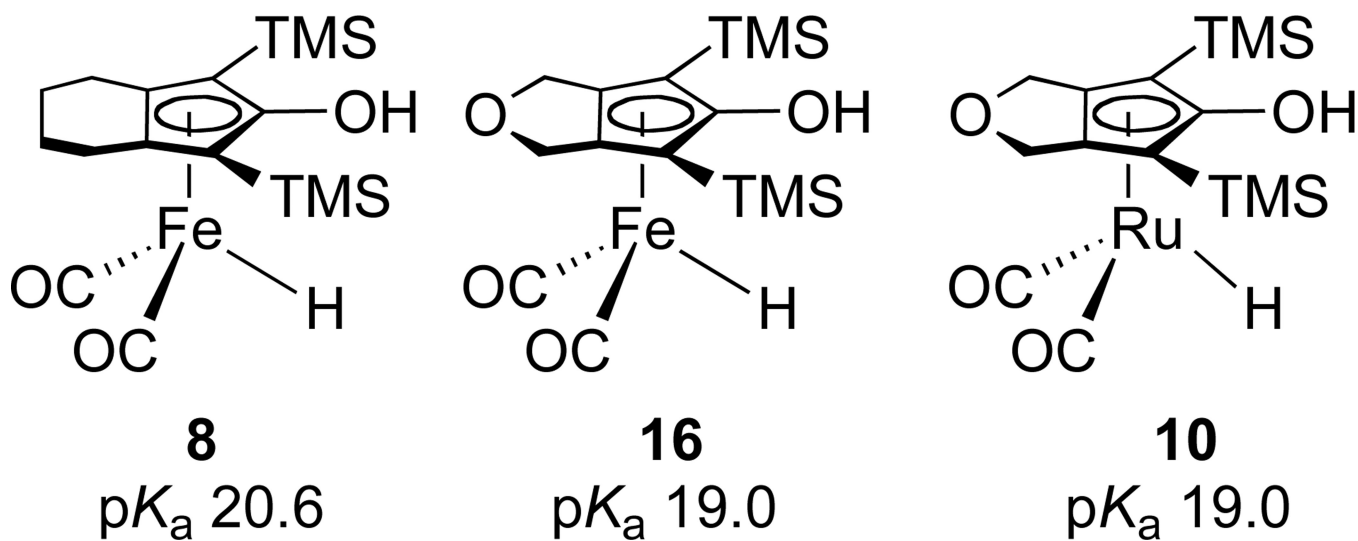
Scheme 6.



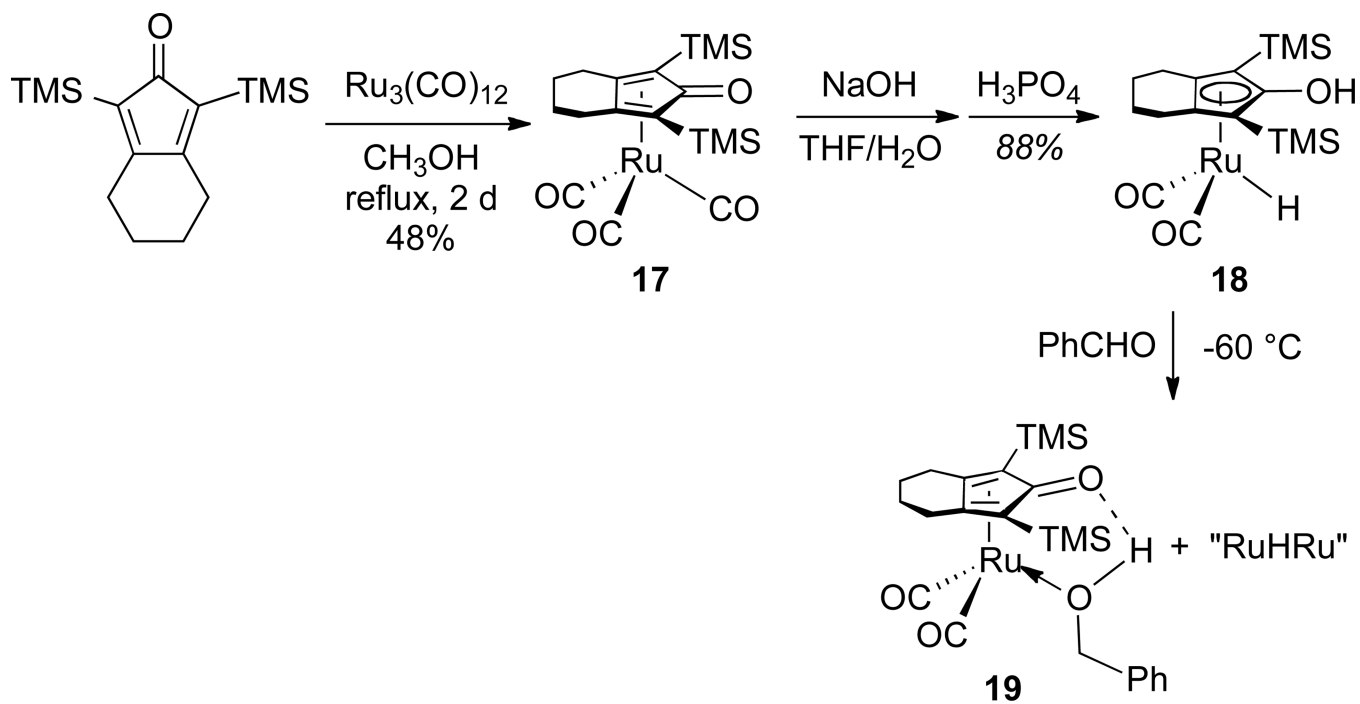
Scheme 7.



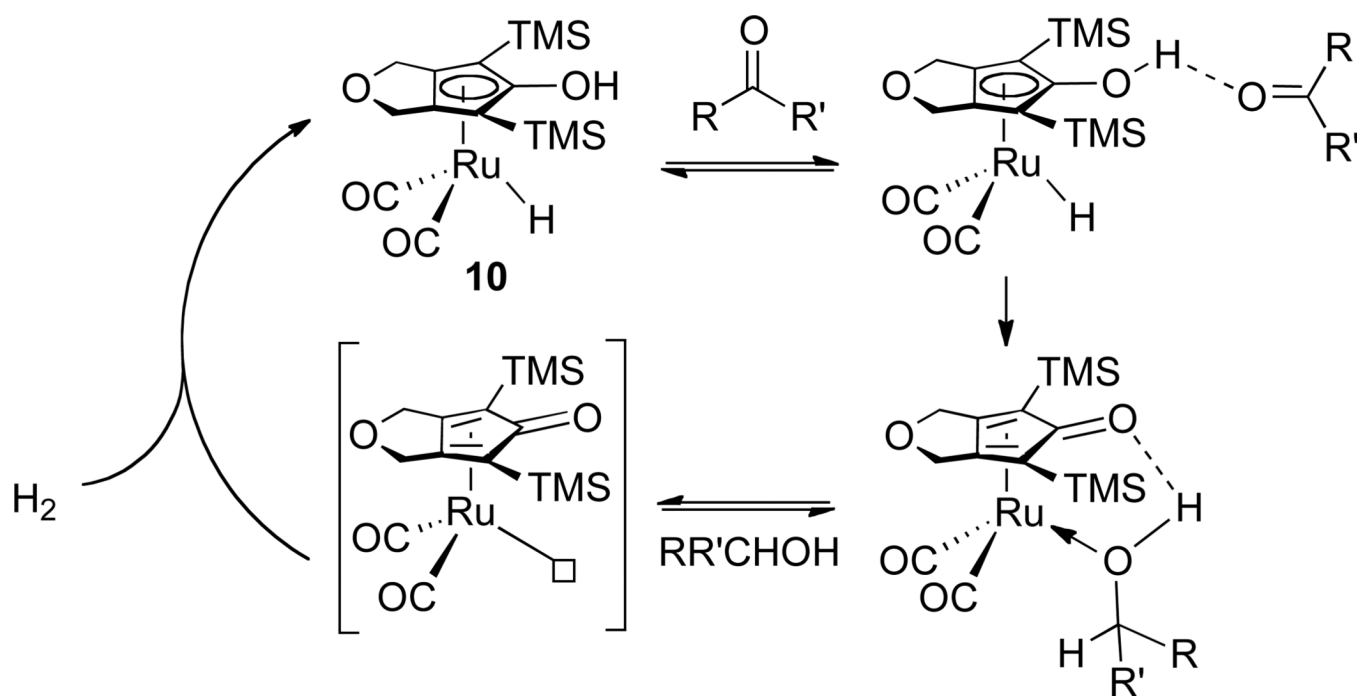
Scheme 8.



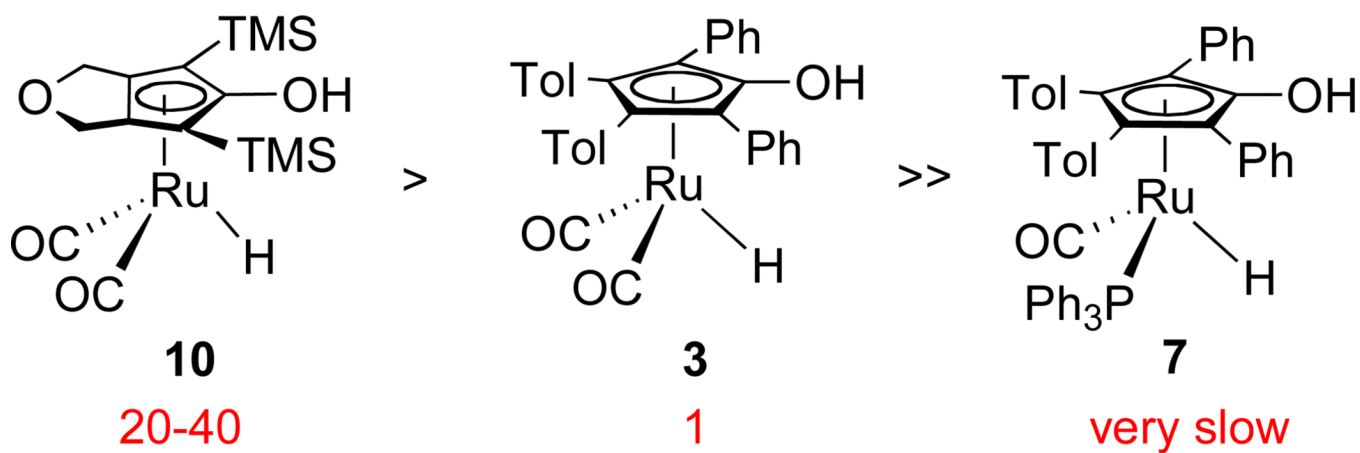
Scheme 9.

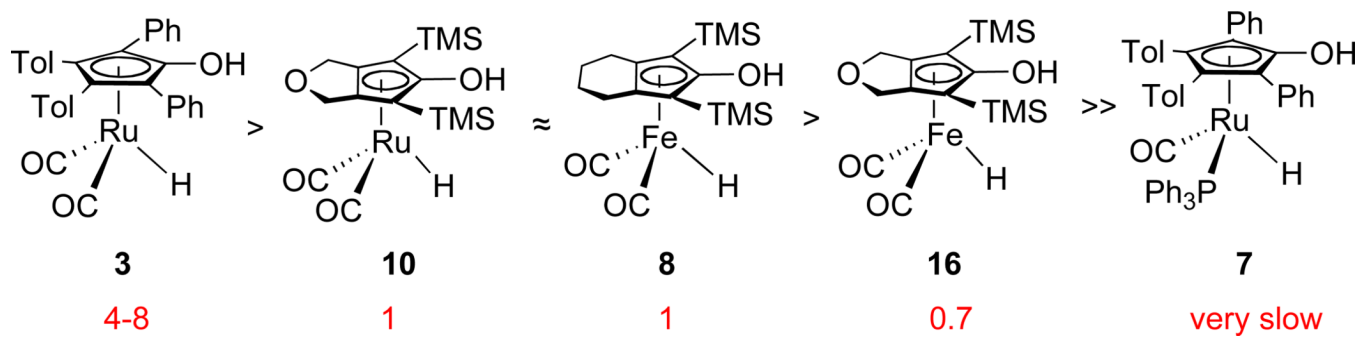


Scheme 10.

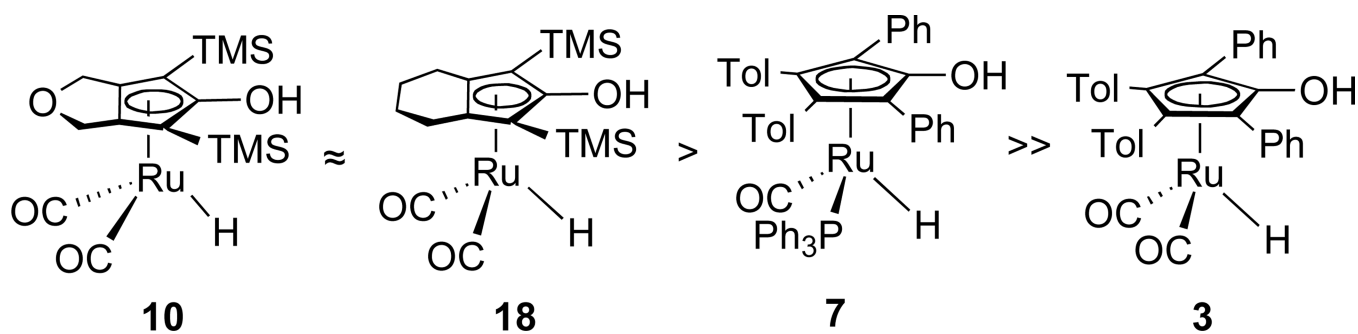


Scheme 11.

**Scheme 12.**Relative activity for stoichiometric PhCHO reduction in toluene- d_8 at -60 °C.

**Scheme 13.**

Relative activity for stoichiometric PhCOCH_3 reduction in toluene- d_8 at 5 °C.

**Scheme 14.**

Relative catalytic activity for the hydrogenation of PhCHO in toluene at 25 °C under 3 atm of H₂ pressure.

Table 1Hydrogenation of Carbonyls Catalyzed by Ruthenium Hydrides **10** and **18** and by Iron Hydride **8**.^a

substrate	catalyst	Time (h)	conversion (%)	yield (%) ^b
PhCHO	10	1	100	91
PhCHO	18	1	100	92
PhCHO	8	1	100	90
PhCOCH ₃	10	20	99	80
PhCOCH ₃	18	24	97	83
PhCOCH ₃	8	20	99	83

^aConditions: [substrate] = 0.30 M, [catalyst] = 0.0060 M, $p(\text{H}_2)$ = 3 atm, in toluene at 25 °C.^bisolated yield.